Proceedings of the ASME 2014 International Design Engineering Technical Conferences & Computers and Information in Engineering Conference
IDETC/CIE 2014
August 17-20, 2014, Buffalo, New York, USA

DETC2014-35374

VEHICLE SUSPENSION DESIGN BASED ON A SIX-BAR LINKAGE

Mark M. Plecnik*
Robotics and Automation Laboratory
Department of Mechanical and Aerospace Engineering
University of California
Irvine, California 92697
Email: mplecnik@uci.edu

J. Michael McCarthy
Robotics and Automation Laboratory
Department of Mechanical and Aerospace Engineering
University of California
Irvine, California 92697
Email: jmmccart@uci.edu

ABSTRACT

A synthesis technique for designing novel vehicle suspension linkages based on the Watt I six-bar is presented. The goal is to maintain near vertical alignment of the wheels to the road during cornering. The complete suspension is analyzed as a symmetric planar 12-bar linkage with ground pivots located at the contact patches. The design procedure specifies the vehicle chassis orientation and the tire camber angles of the vehicle when cornering. As well, two task positions of the wheels with respect to the chassis are specified for suspension movement in straightaways. The result is 18 design equations with 18 unknowns that have a total degree of 2,097,152, though only 336 roots. An example design is presented.

INTRODUCTION

This paper presents the synthesis theory for novel automotive suspension designs based on the Watt I six-bar. The motion objectives of the synthesis are (i) to guide the chassis and wheels of the vehicle into a specified pose when cornering, and (ii) to guide the motion of the wheels through two task positions with respect to the chassis suitable for straightaways. This motion specification is equivalent to solving for four task positions of the wheel with respect to the chassis. In order to specify our motion objective we adopt two planar linkage models. They are a Watt I six-bar with base pivots b and c attached to a fixed chassis (Fig. 1), and a symmetric 12-bar with base pivots N_R and N_L assumed to exist in the middle of the tire contact patches (Fig. 2). The objective of the motion specification is for the wheels to remain near vertical to road during cornering in order to maintain an optimal contact patch. An improved contact patch provides for even tire wear and uniform tire heating. As well, these two performance enhancements can lead to further performance gains including decreased rolling resistance and an increased coefficient of friction through proper heating.

LITERATURE REVIEW

The design of each side of the 12-bar suspension system is based on the kinematic synthesis of a Watt I six-bar linkage for motion generation. The loop equations of this linkage are formulated following Wampler et al. (1992) [1]. Also see, McLarnan (1963) [2] and Kim et al (1973) [3] for early work on six-bar linkage synthesis for function generation and path generation. This work is a generalization of the finite position synthesis problem for four-bar linkages, see Hartenberg and Denavit (1964) [4]. In contrast to Soh and McCarthy (2008) [5], we specify the locations of the ground pivots and the locations of the end-effector pivots, and solve a four position problem.

We solve the synthesis equations using the polynomial homotopy continuation software Bertini, Bates et. al. [6]. This solution was then used in a parameter homotopy to solve the synthesis equations of a Watt I six-bar that travels through four task positions. Our procedure uses tolerance zones to find usable linkages among synthesis solutions that correspond to a ma-

*Address all correspondence to this author.

jority of defective linkages, Plecnik and McCarthy (2012) [7]. Balli and Chand (2002) [8] surveyed the literature on linkage defects. An interesting result is that our formulation yields a reflection defect in which a ternary link of the six-bar needs to be disassembled and reflected in order to move through the entire specified motion. The maximum number of circuits of a Watt mechanism is four, Primrose et al. (1967) [9], but considering assemblies where the ternary link is reflected would increase it to eight. Therefore, synthesis solutions that exhibit this defect are considered to yield multiple linkages.

Dimensional synthesis plays an important role in vehicle suspension design. Sancibrian et al. (2010) [10] applied optimization to design the link lengths of a double-wishbone suspension. Habibi et al. (2008) [11] applied genetic algorithms to the design of linkages based off the McPherson-strut. Simionescu and Beale (2002) [12] and Eberharter (2007) [13] present kinematic synthesis procedures for five-link spatial suspension linkages. Our approach designs the left and right sides of a vehicle suspension as a planar symmetric 12-bar, that is two symmetric Watt I six-bars. Deo and Nam (2004) [14] also propose the design of Watt I six-bar suspension linkages for the purpose of minimizing changes in wheel alignment parameters due to suspension travel.

WATT I SIX-BAR MODEL

The Watt I six-bar model is shown in Fig. 1. Reference frame Γ_A is located at point A attached to the chassis (link I). The complex vectors b and c are measured from reference frame Γ_A and locate the fixed chassis pivots. The vector d locates pivot D in a frame attached to link II which is rotated ρ from Γ_A. The vectors f and g locate pivots F and G in a frame attached to link III which is rotated μ from Γ_A. The task position frame Γ_M is fixed to the tire (link VI) with its origin in the middle of the contact patch and its horizontal axis perpendicular to the side wall of the tire. Its origin is located by M and it is rotated θ from Γ_A. The vectors h and k locate pivots H and K in frame Γ_M.

We do not define vectors that span links IV and V. Instead, we define lengths. The triangle defined by ternary link IV is composed of lengths l_1, l_2, and l_3. Link V is of length l_4.

The motion objective of this six-bar is to move the task position frame attached to the tire through two positions specified by complex vectors M_j and rotations θ_j for $j = 1, 2$. These positions should be specified in order to ensure nearly vertical translation of the tire with respect to the chassis. Along with the tire task frame, we also completely specify the fixed pivots b and c and the end effector pivots h and k.

Our goal is to find the real and imaginary components of d, f, and g and the real numbers l_1, l_2, l_3, and l_4 for a total of 10 design parameters. We shall not solve for the real and imaginary components of complex numbers, but instead solve for the complex numbers and their conjugates directly i.e. the

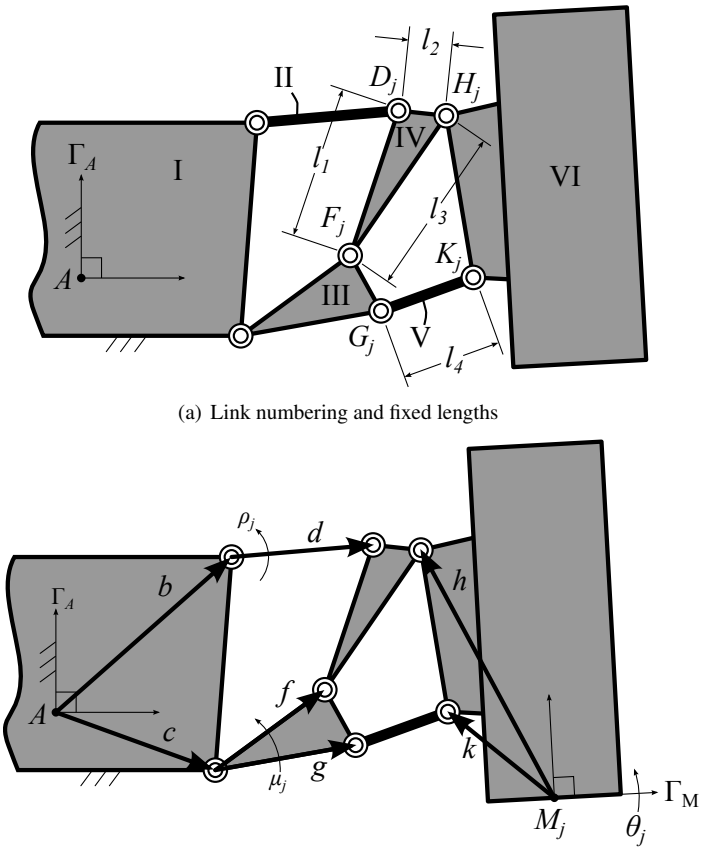

(a) Link numbering and fixed lengths

(b) Vectors and angles

FIGURE 1. (a) LINKS ARE NUMBERED WITH ROMAN NUMERALS. LINKS IV AND V ARE REPRESENTED BY LENGTHS. (b) LINKS I, II, III, VI ARE REPRESENTED BY LOCAL COORDINATE VECTORS.

unknowns are d, $\bar{d}$, f, $\bar{f}$, g, and $\bar{g}$. We treat complex numbers and their conjugates as isotropic coordinates, Wampler et al. (1992) [1].

Since we are using complex numbers to represent planar geometry, we will also be using complex exponential operators to rotate complex numbers. The complex operators for angles ρ_j, μ_j, and θ_j are

$$R_j = e^{i\rho_j}, \qquad U_j = e^{i\mu_j}, \qquad T_j = e^{i\theta_j}, \tag{1}$$

respectively. In order to formulate the synthesis equations, we first derive complex number expressions for points D, F, G, H,

and K measured in frame Γ_A,

$$\begin{aligned} D_j &= b + R_j d \\ F_j &= c + U_j f \\ G_j &= c + U_j g \\ H_j &= M_j + T_j h \\ K_j &= M_j + T_j k \qquad j = 1,2. \end{aligned} \tag{2}$$

Next, we write out four constraint equations per position based on the constant lengths l_1, l_2, l_3, and l_4,

$$\begin{aligned} l_1^2 &= (D_j - F_j)(\bar{D}_j - \bar{F}_j) \\ l_2^2 &= (D_j - H_j)(\bar{D}_j - \bar{H}_j) \\ l_3^2 &= (F_j - H_j)(\bar{F}_j - \bar{H}_j) \\ l_4^2 &= (G_j - K_j)(\bar{G}_j - \bar{K}_j) \qquad j = 1,2. \end{aligned} \tag{3}$$

Without loss of generality, we set $R_1 = \bar{R}_1 = U_1 = \bar{U}_1 = 1$ and append normalization conditions for the remaining rotational operators,

$$R_j \bar{R}_j = 1, \qquad U_j \bar{U}_j = 1, \qquad j = 2. \tag{4}$$

Eqns. (3) and (4) are 10 equations in the 14 unknowns d, $\bar{d}$, f, $\bar{f}$, g, $\bar{g}$, l_1, l_2, l_3, l_4, R_2, $\bar{R}_2$, U_2, and $\bar{U}_2$. This is an underdetermined system. The system becomes determined by considering additional synthesis equations from the 12-bar model (Fig. 2). However, at this point it is worth it to reconsider Eqns. (3) and (4) with a maximum value of $j = 4$ positions. If this were the case, (3) and (4) would represent 22 equations with eight additional rotational unknowns added to those above for a total of 22 unknowns. This determined system could be reduced by subtracting the $j = 1$ equations of (3) from each corresponding equation for all other j in order to eliminate l_1, l_2, l_3, and l_4.

$$\begin{aligned} (D_j - F_j)(\bar{D}_j - \bar{F}_j) - (D_1 - F_1)(\bar{D}_1 - \bar{F}_1) &= 0 \\ (D_j - H_j)(\bar{D}_j - \bar{H}_j) - (D_1 - H_1)(\bar{D}_1 - \bar{H}_1) &= 0 \\ (F_j - H_j)(\bar{F}_j - \bar{H}_j) - (F_1 - H_1)(\bar{F}_1 - \bar{H}_1) &= 0 \\ (G_j - K_j)(\bar{G}_j - \bar{K}_j) - (G_1 - K_1)(\bar{G}_1 - \bar{K}_1) &= 0 \\ R_j \bar{R}_j &= 1 \\ U_j \bar{U}_j &= 1 \qquad j = 2,3,4 \end{aligned} \tag{5}$$

Eqns. (5) have the same structure as Eqns. (12) below and thus the problem presented in this paper is equivalent to four position synthesis of a Watt I six-bar.

THE SYMMETRIC 12-BAR MODEL

In order to specify our motion guidance objectives and obtain additional synthesis equations that can appended to (3) and (4) to create a determined system, we turn to the symmetric 12-bar model as shown in Fig. 2.

The 12-bar model consists of 11 moving links (links I–XI). The right and left tires are links VI and XI and are pinned to the ground at the center of their contact patches. The chassis is link I. The right suspension links are II-V and the left suspension links are VII-X. The left suspension links are a reflection of the right suspension links.

The two fixed pivots are located in reference frame Γ_O by the vectors N and $-\bar{N}$. Note that the reflection of a complex number over the imaginary axis is the negative of its conjugate. As well, frames Γ_{NR} and Γ_{NL} are located at N_R and N_L and aligned with each respective tire. The angular displacements of Γ_{NR} and Γ_{NL} from Γ_O are ψ_R and ψ_L, respectively. Note that Γ_{NR} and Γ_M from Fig. 1 coincide. The vectors h and k locate pivots H_R and K_R in Γ_{NR}. The vectors $-\bar{h}$ and $-\bar{k}$ locate pivots H_L and K_L in Γ_{NL}.

Unlike the six-bar model, the chassis link moves in the 12-bar model. The reference frame Γ_A is fixed to the chassis. It is displaced from Γ_O by translation vector A and angle ϕ. The vectors b, $-\bar{b}$, c, and $-\bar{c}$ locate pivots B_R, B_L, C_R, and C_L in frame Γ_A, respectively. Vector d locates pivot D_R in a link II frame which is rotated by $\phi + \rho_R$ from Γ_O. Vectors f and g locate pivots F_R and G_R in a link III frame which is rotated by $\phi + \mu_R$ from Γ_O. On the left hand side, vector $-\bar{d}$ locates pivot D_L in a link VII frame which is rotated by $\phi + \rho_L$ from Γ_O. Vectors $-\bar{f}$ and $-\bar{g}$ locate pivots F_L and G_L in a link VIII frame which is rotated by $\phi + \mu_L$ from Γ_O.

The 12-bar model allows us to specify a single configuration of the wheels and chassis when the vehicle is cornering. The motion parameters to specify are the camber angles ψ_R and ψ_L, the roll of the chassis ϕ, and the location of chassis reference point A. As well, N is specified to set the vehicle's track, and b, c, h, and k were all specified from the previous six-bar model.

In order to generate the synthesis equations, we first define rotational operators for the new angles ϕ, ρ_R, ρ_L, μ_R, μ_L, ψ_R, ψ_L, that is

$$\begin{aligned} Q = e^{i\phi}, \quad S_R = e^{i\psi_R}, \quad R_R = e^{i\rho_R}, \quad U_R = e^{i\mu_R}, \\ S_L = e^{i\psi_L}, \quad R_L = e^{i\rho_L}, \quad U_L = e^{i\mu_L}. \end{aligned} \tag{6}$$

Next we express points D_R, D_L, F_R, F_L, G_R, G_L, H_R, H_L, K_R, and

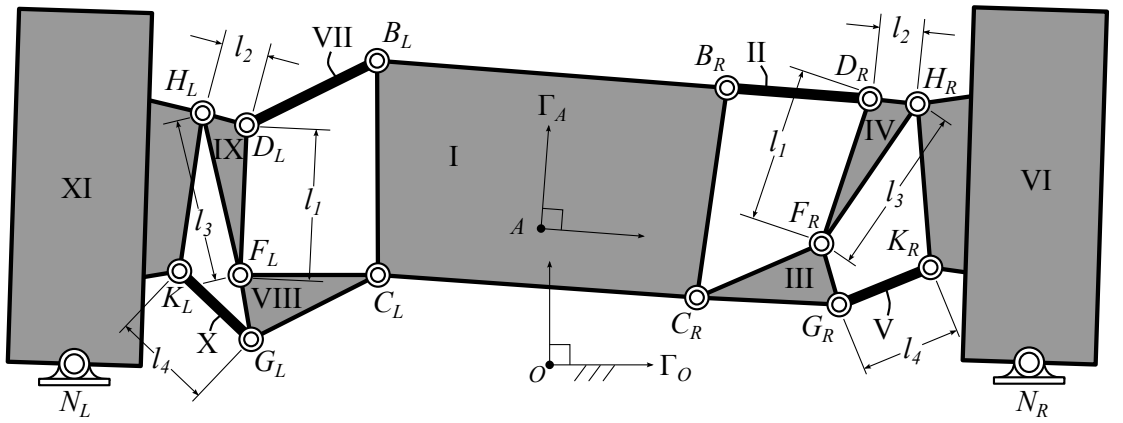

(a) Link numbering and fixed lengths

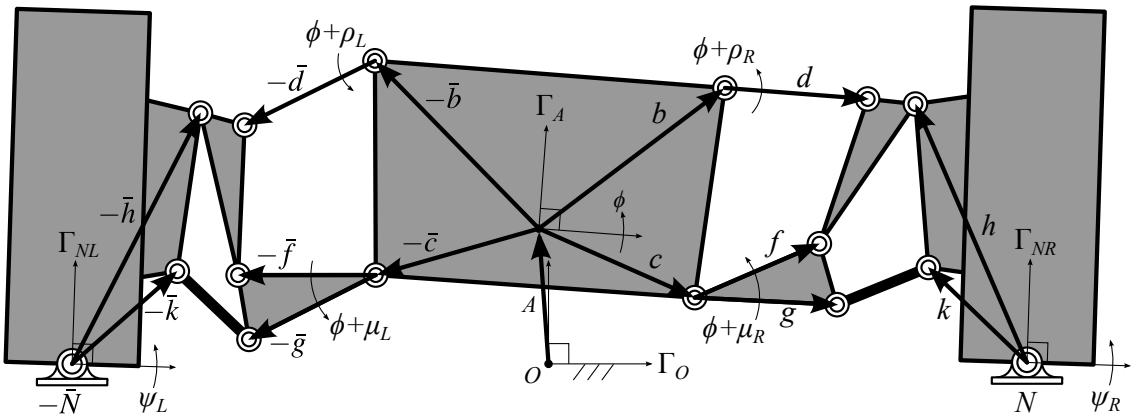

(b) Vectors and angles

FIGURE 2. (a) LINKS IV, V, IX, AND X ARE REPRESENTED BY LENGTHS. (b) LINKS I, II, III, VI, VII, VIII, XI ARE REPRESENTED BY LOCAL COORDINATE VECTORS.

K_L as complex vectors

$$\begin{aligned} D_R &= A + Qb + QR_R d & D_L &= A - Q\bar{b} - QR_L\bar{d} \\ F_R &= A + Qc + QU_R f & F_L &= A - Q\bar{c} - QU_L\bar{f} \\ G_R &= A + Qc + QU_R g & G_L &= A - Q\bar{c} - QU_L\bar{g} \\ H_R &= N + S_R h & H_L &= -\bar{N} - S_L\bar{h} \\ K_R &= N + S_R k & K_L &= -\bar{N} - S_L\bar{k} \end{aligned} \tag{7}$$

and formulate eight constraint equations based of the lengths that compose links III, IV, VIII, and IX,

$$\begin{aligned} l_1^2 &= (D_R - F_R)(\bar{D}_R - \bar{F}_R) & l_1^2 &= (D_L - F_L)(\bar{D}_L - \bar{F}_L) \\ l_2^2 &= (D_R - H_R)(\bar{D}_R - \bar{H}_R) & l_2^2 &= (D_L - H_L)(\bar{D}_L - \bar{H}_L) \\ l_3^2 &= (F_R - H_R)(\bar{F}_R - \bar{H}_R) & l_3^2 &= (F_L - H_L)(\bar{F}_L - \bar{H}_L) \\ l_4^2 &= (G_R - K_R)(\bar{G}_R - \bar{K}_R) & l_4^2 &= (G_L - K_L)(\bar{G}_L - \bar{K}_L). \end{aligned} \tag{8}$$

By appending normalization conditions for the unknown angle variables

$$R_R\bar{R}_R = 1, \quad R_L\bar{R}_L = 1, \quad U_R\bar{U}_R = 1, \quad U_L\bar{U}_L = 1, \tag{9}$$

we obtain 12 equations in 18 unknowns, an underdetermined system. However, by combining Eqns. (3), (4), (8), (9), we form a system of 22 equations in the 22 unknowns

$$\{d, \bar{d}, f, \bar{f}, g, \bar{g}, l_1, l_2, l_3, l_4\} \quad \text{and} \quad \{R_j, \bar{R}_j, U_j, \bar{U}_j\} \quad j = 2, R, L. \tag{10}$$

Combining the constraint equations from (3) and (8), we obtain

$$\begin{aligned} l_1^2 &= (D_j - F_j)(\bar{D}_j - \bar{F}_j) \\ l_2^2 &= (D_j - H_j)(\bar{D}_j - \bar{H}_j) \\ l_3^2 &= (F_j - H_j)(\bar{F}_j - \bar{H}_j) \\ l_4^2 &= (G_j - K_j)(\bar{G}_j - \bar{K}_j) \qquad j = 1,2,R,L. \end{aligned} \tag{11}$$

This system can be reduced by subtracting the $j = 1$ equations from each corresponding equation $j = 2,R,L$ in order to eliminate l_1, l_2, l_3, and l_4. Completing this operation, we obtain our 18 final synthesis equations in 18 unknowns,

$$\begin{aligned} \mathcal{S}_{1j} &: (D_j - F_j)(\bar{D}_j - \bar{F}_j) - (D_1 - F_1)(\bar{D}_1 - \bar{F}_1) = 0 \\ \mathcal{S}_{2j} &: (D_j - H_j)(\bar{D}_j - \bar{H}_j) - (D_1 - H_1)(\bar{D}_1 - \bar{H}_1) = 0 \\ \mathcal{S}_{3j} &: (F_j - H_j)(\bar{F}_j - \bar{H}_j) - (F_1 - H_1)(\bar{F}_1 - \bar{H}_1) = 0 \\ \mathcal{S}_{4j} &: (G_j - K_j)(\bar{G}_j - \bar{K}_j) - (G_1 - K_1)(\bar{G}_1 - \bar{K}_1) = 0 \\ \mathcal{N}_{1j} &: R_j \bar{R}_j = 1 \\ \mathcal{N}_{2j} &: U_j \bar{U}_j = 1 \qquad j = 2,R,L. \end{aligned} \tag{12}$$

REDUCTION OF SYNTHESIS EQUATIONS

An expansion of the polynomials of (12) reveals the monomial structure,

$$\begin{aligned} \mathcal{S}_{1j} &: \langle d,\bar{d},1\rangle \langle f,\bar{f},1\rangle \langle R_j,\bar{R}_j,1\rangle \langle U_j,\bar{U}_j,1\rangle \\ \mathcal{S}_{2j} &: \langle d,\bar{d},1\rangle \langle R_j,\bar{R}_j,1\rangle \\ \mathcal{S}_{3j} &: \langle f,\bar{f},1\rangle \langle U_j,\bar{U}_j,1\rangle \\ \mathcal{S}_{4j} &: \langle g,\bar{g},1\rangle \langle U_j,\bar{U}_j,1\rangle \\ \mathcal{N}_{1j} &: \langle R_j,\bar{R}_j,1\rangle^2 \\ \mathcal{N}_{2j} &: \langle U_j,\bar{U}_j,1\rangle^2 \qquad j = 2,R,L. \end{aligned} \tag{13}$$

from which we compute a total degree $(4 \times 2^5)^3 = 2,097,152$. However, from (13), we see that the variables of (12) are naturally split into the nine groups

$$\begin{array}{lll} \text{Gr 1: } \langle d,\bar{d}\rangle & \text{Gr 4: } \langle R_2,\bar{R}_2\rangle & \text{Gr 7: } \langle U_R,\bar{U}_R\rangle \\ \text{Gr 2: } \langle f,\bar{f}\rangle & \text{Gr 5: } \langle U_2,\bar{U}_2\rangle & \text{Gr 8: } \langle R_L,\bar{R}_L\rangle \\ \text{Gr 3: } \langle g,\bar{g}\rangle & \text{Gr 6: } \langle R_R,\bar{R}_R\rangle & \text{Gr 9: } \langle U_L,\bar{U}_L\rangle \end{array} \tag{14}$$

We compute the 9-homogeneous Bezout number (Morgan and Sommese (1987) [15]) for this system as the coefficient of the monomial $\alpha_1^2\alpha_2^2\alpha_3^2\alpha_4^2\alpha_5^2\alpha_6^2\alpha_7^2\alpha_8^2\alpha_9^2$ in the polynomial

$$\begin{aligned} &(\alpha_1+\alpha_2+\alpha_4+\alpha_5)(\alpha_1+\alpha_4)(\alpha_2+\alpha_5)(\alpha_3+\alpha_5)2\alpha_4 2\alpha_5 \\ &(\alpha_1+\alpha_2+\alpha_6+\alpha_7)(\alpha_1+\alpha_6)(\alpha_2+\alpha_7)(\alpha_3+\alpha_7)2\alpha_6 2\alpha_7 \\ &(\alpha_1+\alpha_2+\alpha_8+\alpha_9)(\alpha_1+\alpha_8)(\alpha_2+\alpha_9)(\alpha_3+\alpha_9)2\alpha_8 2\alpha_9 \end{aligned} \tag{15}$$

which is 3840.

The number of roots can then be reduced even further by use of parameter homotopy of which an implementation is available in the Bertini software package. The idea behind the parameter homotopy numerical reduction method is to solve a system generally once by assigning random complex numbers to the parameters which comprise the coefficients of the polynomial system (12). The number of nonsingular solutions from this general continuation solve is taken to be the maximum number of nonsingular roots of the system. These nonsingular solutions can be combined with the previously randomly generated parameters to construct straight line homotopies which only need to track the reduced number of paths associated with the nonsingular roots of the system.

We completed the following numerical reduction on a Mac Pro with 12×2.93 GHz processors running in parallel. The parameters are the 26 variables which contain information of the specified pivots and motion of the mechanism. They are

$$\begin{aligned} &\{A,\bar{A},b,\bar{b},c,\bar{c},h,\bar{h},k,\bar{k},M_1,\bar{M}_1,M_2,\bar{M}_2, \\ &N,\bar{N},Q,\bar{Q},S_R,\bar{S}_R,S_L,\bar{S}_L,T_1,\bar{T}_1,T_2,\bar{T}_2\}. \end{aligned} \tag{16}$$

Eqns. (12) were 9-homogenized and solved generally by Bertini to find 336 nonsingular solutions from 3840 paths. This computation took 13 minutes. Subsequent solutions tracked 336 paths and only took 10-12 seconds on our parallelized system.

LINKAGE ANALYSIS

The above reduction shows a maximum of 336 linkage solutions that can be found for a set of synthesis equations (12). However, for a single set of specified chassis and wheel mounting pivots, we can generate four sets of synthesis equations by swapping the values of b and c, and h and k as illustrated in Fig. 3. Therefore, for a single specification of the pivots and motion, we will not find more than 1344 linkage solutions. However, the large majority of these solutions are either not physically realizable or suffer from a variety of linkage defects including order, branch, and circuit.

Our synthesis procedure also yields a reflection defect, which occurs when a link of the mechanism needs to be disassembled and flipped in order to reach all specified poses. The

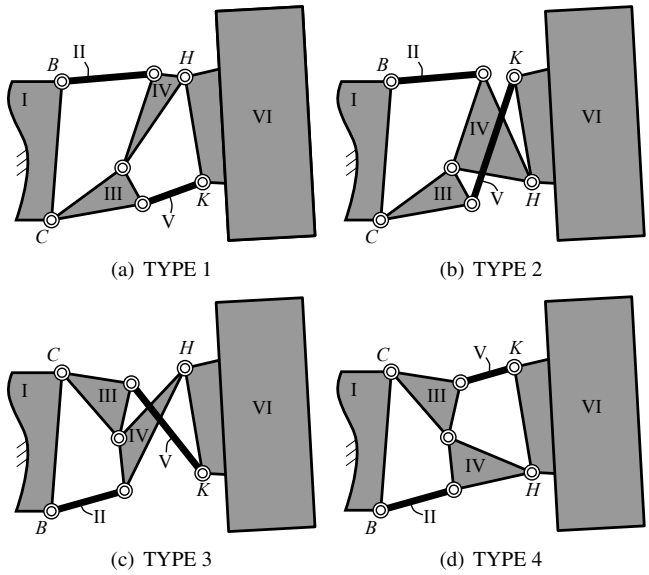

FIGURE 3. THERE ARE FOUR DIFFERENT WAYS TO ASSIGN COORDINATES TO b, c, h, AND k AND STILL HAVE GROUND AND END EFFECTOR PIVOTS AT THE SAME LOCATIONS.

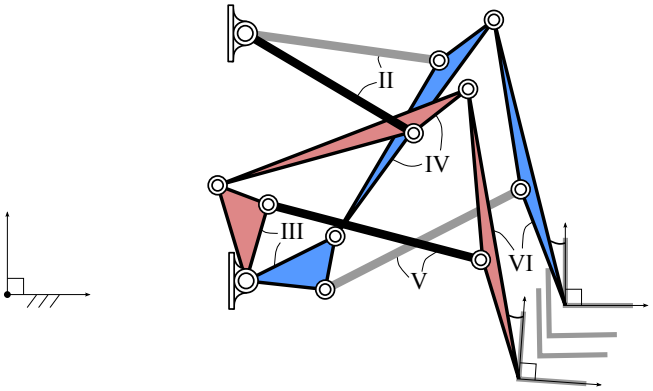

FIGURE 4. THIS LINKAGE SHOWS LINK IV RELFECTED BETWEEN TASK POSITIONS. THIS IS AN ASSEMBLY DEFECT, WE CALL A *REFLECTION DEFECT*.

presence of this defect stems from the fact that the shape of ternary links IV and IX are represented by the three lengths l_1, l_2, and l_3. These three lengths can be assembled into two different triangles which are reflected versions of each other. Note on the other hand, links III and VIII cannot suffer from reflection defects because their shapes are uniquely specified by vectors measured from their local link frames.

We illustrate a reflection defect in Fig. 4. The dimensions of

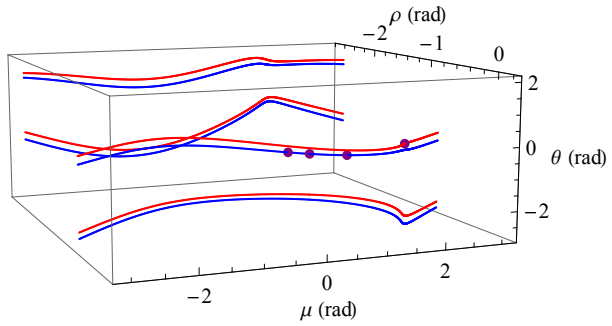

FIGURE 5. THE REFLECTION OF THE TERNARY LINK IV YIELDS PAIRS OF ASSOCIATED CIRCUITS SHOWN AS RED AND BLUE. THE FOUR TASK POSITIONS ARE SHOWN AS POINTS ON THESE CIRCUITS.

this mechanism are

$$
\begin{aligned}
&b = 12 + 13.25i, \quad c = 12 + 0.75i,\\
&d = 9.36337843789255 - 3.093764412396068i,\\
&f = 4.992554906665183 + 0.05422889589565189i,\\
&g = 3.367084128230273 - 2.219778384337775i,\\
&h = -3.11 + 14.5i, \quad k = -2.06 + 6i,\\
&l_1 = 10.322990240375162, \quad l_2 = 3.406229534641514,\\
&l_3 = 13.528194647225071, \quad l_4 = 11.134005416892984 \quad (17)
\end{aligned}
$$

and it was solved for using the untoleranced motion requirement in Table 1. Link IV of this mechanism must have its orientation reflected in order to reach the final specified pose.

Fig. 5 illustrates the circuits of this mechanism in the configuration space (ρ, μ, θ) where μ is seen to be fully rotatable. The red and blue circuits correspond with the red and blue orientations of link IV in Fig. 4. The purple points mark configurations that correspond to task positions and are split between red and blue circuits.

The Watt I linkage has at most four circuits (Primrose et al. [9]), therefore we conclude that the mechanism configurations with a reflected coupler link corresponds to a different linkage. From this point of view, a synthesis solution with a reflection defect is yielding two linkage designs in order to complete a single set of tasks. This linkage cannot reach all poses and is not usable.

FORWARD KINEMATICS

In order to filter out linkages that are kinematically defective, we simulate the geometric motion of all linkage solutions. This is accomplished by formulating and solving the forward kinematics equations of the six-bar (Fig. 1) and 12-bar (Fig. 2) models.

In order to formulate and solve the forward kinematics for the six-bar and 12-bar models of this suspension, we must choose the input parameter that is representative of the forces and torques on the system. In the case of the six-bar linkage, we use the vertical movement of the tire. And for the 12-bar model, we use the horizontal movement of the chassis. Kinematic analysis also provides the location of singularities, which can be used to quickly filter defective linkages.

Watt I Forward Kinematics

The Watt I model is shown in Fig. 1. For this analysis we chose the vertical component of vector M to be the input parameter. This assumes that the force of the road on the tire will dominate the mechanism's motion. The Watt I constraint equations (3) are re-purposed in order to accommodate forward kinematics,

$$\begin{aligned} l_1^2 &= (D-F)(\bar{D}-\bar{F}) \\ l_2^2 &= (D-H)(\bar{D}-\bar{H}) \\ l_3^2 &= (F-H)(\bar{F}-\bar{H}) \\ l_4^2 &= (G-K)(\bar{G}-\bar{K}). \end{aligned} \tag{18}$$

Expanding these equations and appending normalization conditions for the angular operator unknowns, we obtain

$$\begin{aligned} l_1^2 &= (b+Rd-c-Uf)(\bar{b}+\bar{R}\bar{d}-\bar{c}-\bar{U}\bar{f}) \\ l_2^2 &= (b+Rd-M-Th)(\bar{b}+\bar{R}\bar{d}-\bar{M}-\bar{T}\bar{h}) \\ l_3^2 &= (c+Uf-M-Th)(\bar{c}+\bar{U}\bar{f}-\bar{M}-\bar{T}\bar{h}) \\ l_4^2 &= (c+Ug-M-Tk)(\bar{c}+\bar{U}\bar{g}-\bar{M}-\bar{T}\bar{k}) \\ R\bar{R} &= 1 \\ U\bar{U} &= 1 \\ T\bar{T} &= 1. \end{aligned} \tag{19}$$

That is seven equations in eight unknowns, a one DOF system. The unknowns are the three angular variables, their conjugates, and M, $\bar{M}$. Next we define the imaginary component of M as M_y. M_y shall be the specified input, we introduce it to the system by appending the isotropic transformation,

$$M_y = \frac{1}{2i}(M-\bar{M}) \tag{20}$$

With M_y specified, Eqns. (19) and (20) are eight equations in eight unknowns.

The forward kinematics equations are used to build mechanism trajectories by solving these equations over a sequence of heights M_y. The forward kinematics equations were solved using the Newton-Raphson based FindRoot solver of the Mathematica software package. Trajectories were established by first solving for the configuration at $j = 1$, using R_1, $\bar{R}_1$, U_1, $\bar{U}_1$, T_1, $\bar{T}_1$, M_1, $\bar{M}_1$ as specified during the synthesis as a starting point. Then, M_y was incremented and the forward kinematics were solved again using the previous configuration as a starting point. M_y was incremented upwards until a singular configuration was encountered. At that point, we returned to the $j = 1$ configuration and M_y was incremented downwards until a singular configuration was encountered. Piecing these two trajectories together, we create a mechanism branch that travels from one singular configuration to another. Our algorithm detects singularities by checking if the rotational operators have unit magnitude. If they do not have unit magnitude, then the mechanism is not in a physically realizable configuration and the trajectory has moved beyond a singular point.

Each configuration of the resulting mechanism branch is represented by a forward kinematics solution set $\{R,\bar{R},U,\bar{U},T,\bar{T},M,\bar{M}\}$. However, by this point we have ensured that unknowns and their barred counterparts are indeed conjugates. So we represent each configuration by the set $\{R,U,T,M\}$. Next, we check if the configurations associated with the specified task positions of the synthesis portion are present within the mechanism branch.

The two task positions are defined by the rotational operators T_1 and T_2, and the translation vectors M_1 and M_2. The corresponding task configurations are $\{R_1,U_1,T_1,M_1\}'$ and $\{R_2,U_2,T_2,M_2\}'$. Note that the prime notation was added to distinguish between configurations specified by the motion requirement and configurations found from the forward kinematics equations. Because of the chosen Newton-Raphson starting point, we are always analyzing the branch in which $\{R_1,U_1,T_1,M_1\}'$ is present.

12-Bar Forward Kinematics

The symmetric 12-bar model is shown in Fig. 2. For this analysis we chose the horizontal component of vector A to be the input parameter. This assumes that the centripetal force generated by cornering will dominate the mechanism's motion. The 12-bar constraint equations (8) are re-purposed in order to accommodate the forward kinematics. Expanding Eqn. (8) and appending normalization conditions for the rotational operator unknowns, we obtain

$$\begin{aligned} l_1^2 &= (b+R_Rd-c-U_Rf)(\bar{b}+\bar{R}_R\bar{d}-\bar{c}-\bar{U}_R\bar{f}) \\ l_2^2 &= (A+Qb+QR_Rd-N-S_Rh)(\bar{A}+\bar{Q}\bar{b}+\bar{Q}\bar{R}_R\bar{d}-\bar{N}-\bar{S}_R\bar{h}) \\ l_3^2 &= (A+Qc+QU_Rf-N-S_Rh)(\bar{A}+\bar{Q}\bar{c}+\bar{Q}\bar{U}_R\bar{f}-\bar{N}-\bar{S}_R\bar{h}) \\ l_4^2 &= (A+Qc+QU_Rg-N-S_Rk)(\bar{A}+\bar{Q}\bar{c}+\bar{Q}\bar{U}_R\bar{g}-\bar{N}-\bar{S}_R\bar{k}) \end{aligned} \tag{21}$$

$$
\begin{aligned}
l_1^2 &= (-\bar{b} - R_L\bar{d} + \bar{c} + U_L\bar{f})(-b - \bar{R}_L d + c + \bar{U}_L f) \\
l_2^2 &= (A - Q\bar{b} - QR_L\bar{d} + \bar{N} + S_L\bar{h})(\bar{A} - \bar{Q}b - \bar{Q}\bar{R}_L d + N + \bar{S}_L h) \\
l_3^2 &= (A - Q\bar{c} - QU_L\bar{f} + \bar{N} + S_L\bar{h})(\bar{A} - \bar{Q}c - \bar{Q}\bar{U}_L f + N + \bar{S}_L h) \\
l_4^2 &= (A - Q\bar{c} - QU_L\bar{g} + \bar{N} + S_L\bar{k})(\bar{A} - \bar{Q}c - \bar{Q}\bar{U}_L g + N + \bar{S}_L k)
\end{aligned} \tag{22}
$$

$$
\begin{aligned}
Q\bar{Q} &= 1 \\
R_R\bar{R}_R &= 1 \\
U_R\bar{U}_R &= 1 \\
S_R\bar{S}_R &= 1 \\
R_L\bar{R}_L &= 1 \\
U_L\bar{U}_L &= 1 \\
S_L\bar{S}_L &= 1.
\end{aligned} \tag{23}
$$

That is 15 equations in 16 unknowns, a one DOF system. The unknowns are the seven angular variables, their conjugates, and A, $\bar{A}$. Next we define the real component of A as A_x. A_x shall be the specified input. We introduce it to the system by appending the isotropic transformation,

$$
A_x = \frac{1}{2}(A + \bar{A}). \tag{24}
$$

With A_x specified, Eqns. (21) through (24) are 16 equations in 16 unknowns.

The forward kinematics equations are used to build mechanism trajectories in the same manner as described for the Watt I. Initially, the FindRoot solver was used to solve these equations using the specified motion configuration $\{A, Q, R_R, U_R, S_R, R_L, U_L, S_L\}'$ from the synthesis portion as a starting point. Then, A_x was incremented and the forward kinematics were solved again using the previous configuration as a starting point. A_x was incremented to the right until a singular configuration was encountered. At that point, we returned to the synthesis configuration $\{A, Q, R_R, U_R, S_R, R_L, U_L, S_L\}'$ and incremented to the left until a singular configuration was encountered.

These two trajectories are pieced together to obtain a mechanism branch that travels from one singular configuration to another. Our algorithm detects singularities by checking if the angular operators have unit magnitude. If they do not have unit magnitude, then the mechanism is not in a physically realizable configuration and the trajectory has moved beyond a singular point.

Each configuration of the resulting mechanism branch is represented by a forward kinematics solution set $\{A, Q, R_R, U_R, S_R, R_L, U_L, S_L\}$. We know that the configuration specified by the motion requirement, that is $\{A, Q, R_R, U_R, S_R, R_L, U_L, S_L\}'$, is present in the mechanism branch because we used it as a starting point to establish that branch. However, we must now ensure that the linkage could move smoothly into the reflected version of the configuration specified by the motion requirement, that is $\{-\bar{A}, \bar{Q}, \bar{R}_L, \bar{U}_L, \bar{S}_L, \bar{R}_R, \bar{U}_R, \bar{S}_R\}'$. The presence of this configuration in the mechanism branch ensures that the mechanism can move into a neutral ($Q = 1$) position. In the neutral configuration, the left suspension linkage will be a mirror image of the right suspension linkage.

Corroborating Six-bar and 12-bar Designs

The final portion of the linkage analysis routine is to ensure the right and left suspension linkages of the 12-bar model move through configurations that correspond to the mechanism branch found when analyzing the six-bar model. In other words, there is no disassembly required to transition between vertical motion of the tire with respect to the chassis, and the cornering motion of the chassis and tires.

The motion specification on the 12-bar can be written as two more task position specifications on the six-bar. The rotational operators and translations of these two additional tasks can be written

$$
\begin{aligned}
T_3 &= \bar{Q}S_R, & M_3 &= \bar{Q}(N - A), \\
T_4 &= Q\bar{S}_L, & M_4 &= Q(N + \bar{A}).
\end{aligned} \tag{25}
$$

We can then check to see whether the configurations $\{R_R, U_R, T_3, M_3\}'$ and $\{\bar{R}_L, \bar{U}_L, T_4, M_4\}'$ are present in the six-bar mechanism branch computed from (19).

TOLERANCE ZONES

The procedure outlined above is based off a single specification of pivots and task information. However, it is often the case that no useful linkage designs will result from a single set of specifications. Meanwhile, slightly tweaked sets of specifications may exist that do result in useful designs but finding these specifications is a challenge. We confront this challenge with a random search method inside tolerance zones as used in Plecnik and McCarthy (2012) [7].

DESIGN OF THE SUSPENSION MECHANISM

The idea behind our novel mechanism design is to improve the tire contact patch during cornering. A well distributed contact patch promotes even wear and uniform heating from the inside to the outside of the tire. Tire temperature is critical because it effects the coefficient of friction between the tires and road. As well, tires that have a well managed contact patch can be inflated to higher pressures which helps reduce rolling resistance.

TABLE 1. THE SPECIFIED MOTION REQUIREMENT AND TOLERANCE ZONES. ALL COMPLEX COMPONENTS ARE ASSOCIATED WITH REAL LENGTHS IN INCHES.

	Re	Tolerance	Im	Tolerance
$b^{\dagger}$	12	$-0,+4$	13.25	$-3,+3$
$c^{\dagger}$	12	$-0,+4$	0.75	$-0,+3$
$h^{\ddagger}$	-3.11	$-4,+0$	14.5	$-2,+0$
$k^{\ddagger}$	-2.06	$-4,+0$	6	$-0,+2$
M_1	27.25	± 0.25	-2	± 0.25
θ_1	1°	$\pm 0.25^{\circ}$	n/a	n/a
M_2	26.75	± 0.25	-3	± 0.25
θ_2	1°	$\pm 0.25^{\circ}$	n/a	n/a
A	-1	± 0.5	2.5	± 0.5
ϕ	-4°	$\pm 1^{\circ}$	n/a	n/a
ψ_R	-2°	$\pm 0.25^{\circ}$	n/a	n/a
ψ_L	-2°	$\pm 0.25^{\circ}$	n/a	n/a
N	27	± 0	0	± 0

†Values of b and c are swapped to form different types.

‡Values of h and k are swapped to form different types.

TABLE 2. RESULTS OVER 40 ITERATIONS.

(a) Average solutions over 40 iterations.

	Nonsingular Solutions	Phys. Real	Useful
Type 1	192.55	60.65	0.45
Type 2	190.98	57.93	0.18
Type 3	189.80	68.75	0.23
Type 4	191.05	71.30	0.15
All types	764.38	258.63	1.00

(b) Total number of solutions over 40 iterations.

	Nonsingular Solutions	Phys. Real	Useful
Type 1	7702	2426	18
Type 2	7639	2317	7
Type 3	7592	2750	9
Type 4	7642	2852	6
All types	30,575	10,345	40

A useful linkage found by our algorithm is pictured in Fig. 6 and is helpful to describe the motivation behind the motion requirements. Figs. 6(a) and 6(b) show the specified configurations of the wheels and chassis when the vehicle is turning right and left, respectively. The idea is that the camber of the outside wheel will go slightly negative and the camber of the inside wheel will go slightly positive in order to counter the friction forces of the road on the tires that create a moment in the opposite direction. At the same time, since we assumed that the horizontal centripetal force acting on the center of mass will play a big role, we specify the chassis to move slightly to the outside when cornering, in order to promote actuation of the mechanism by centripetal loads. This made it natural to lean the chassis into the turn as well since leaning the chassis into the turn influenced a smoother set of equivalent four task positions as can be seen Figs. 6(c)–6(f). These figures also reveals the trade-off we encountered. By specifying the 12-bar model in the manner above, we require the wheel to move slightly away from the chassis in its upward movement. This motion can create undesirable effects with respect to straight line stability during bump response.

The motion requirements and tolerances were specified as shown in Table 1. Our algorithm was run for 40 iterations on a Mac Pro with 12×2.93 GHz processors running in parallel. For each iteration, the synthesis portion tracked 336 paths four times for each mechanism type (Fig. 3) in 10-12 seconds via the parameter homotopy module built in to the Bertini software. The analysis portion of each iteration took on average 62 seconds. Therefore, each iteration took about 106 seconds. The results summarized in Table 2 computed in under 70 minutes.

Our algorithm delivered 40 defect-free designs. It is then up to the designer to review this list and cast out those with pivots in inconvenient locations. As well, Table 2(a) shows that on average about 1 in 760 solutions correlate to a usable design.

The methods described in this paper are kinematic and describe a procedure to find the link lengths of a six-bar suspension linkage that moves the chassis and wheels in a particular way. The next step in the design procedure involves designing the springs, dampers, and their mounting points. The challenge of this is to ensure the suspension moves in the desired manner when external loads are applied. That work is out of the scope of this paper.

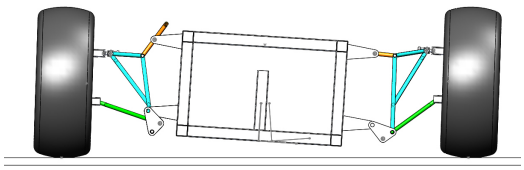

(a) 12-bar Pose 1

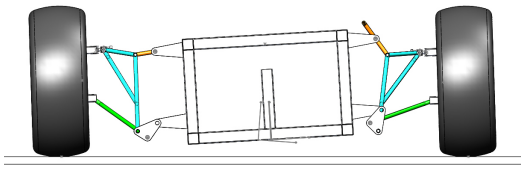

(b) 12-bar Pose 2

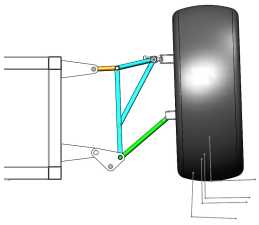

(c) Six-bar Pose 1

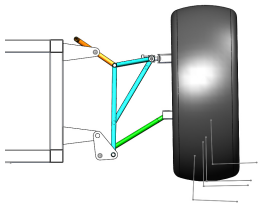

(d) Six-bar Pose 2

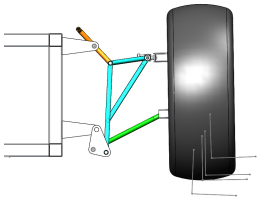

(e) Six-bar Pose 3

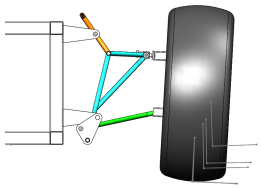

(f) Six-bar Pose 4

FIGURE 6. THE SIX-BAR MODEL. NOTATION HAS BEEN SPLIT INTO TWO FIGURES FOR LEGIBILITY.

CONCLUSION

We have presented a procedure for the kinematic synthesis and analysis of a Watt I six-bar linkage for use as a vehicle suspension. The motion specification and analysis routine utilized in this paper made use of both Watt I six-bar and symmetric 12-bar models. Our approach reduces to four task position synthesis of a Watt I six-bar where both ground pivots and end effector pivots are specified.

The synthesis equations (12) have a total degree of 2,097,152. A 9-homogeneous formulation of the system and the implementation of parameter homotopy in Bertini results in a system with 336 roots is solved in 10 seconds.

We embedded our six-bar linkage synthesis in a 12-bar model in order to facilitate our analysis procedure. The 12-bar model provided a means to filter solutions that do not move smoothly through required symmetric configurations specified for the suspension.

We are in the process building a scale model, defining spring supports, and evaluating the dynamic performance of this six-bar suspension.

ACKNOWLEDGMENT

The authors gratefully acknowledge the support of National Science Foundation award CMMI-1066082. Any opinions, findings, and conclusions or recommendations expressed in this material are those of the authors) and do not necessarily reflect the views of the National Science Foundation.

REFERENCES

[1] C. W. Wampler, A. J. Sommese, and A. P. Morgan, 1992. "Complete solution of the nine-point path synthesis problem for four-bar linkages," *Journal of Mechanical Design*, 114(1):153-159.

[2] C. W. McLarnan, 1963. "Synthesis of six-link plane mechanisms by numerical analysis," *Journal of Engineering for Industry*, 85(1):5-10.

[3] H. S. Kim, S. Hamid, and A. H. Soni, 1973. "Synthesis of six-link mechanisms for point path generation," *Journal of Mechanisms*, 6:447-461.

[4] R. S. Hartenberg and J. Denavit, 1964. *Kinematic Synthesis of Linkages*, McGraw-Hill, New York, NY.

[5] G. S. Soh and J. M. McCarthy, 2008. "The synthesis of six-bar linkages as constrained planar 3R chains," *Mechanism and Machine Theory*, 43(2):160-170.

[6] D. J. Bates, J. D. Hauenstein, A. J. Sommese, and C. W. Wampler, 2013. *Numerically Solving Polynomial Systems with Bertini*, SIAM, Philadelphia, PA.

[7] M. Plecnik and J. M. McCarthy, 2012. "Design of a 5-SS spatial steering linkage," Proceedings of the ASME 2012 IDETC/CIE Conference, Paper No. DETC2012-71405, August 12-15, 2014, Chicago, Illinois.

[8] S. S. Balli and S. Chand, 2002. "Defects in link mechanisms and solution rectification," *Mechanism and Machine Theory*, 37(9):851-876.

[9] E. J. Primrose, F. Freudenstein, and B. Roth, 1967. "Six-bar motion: I. The Watt mechanism," *Archive for Rational Mechanics and Analysis*, 24(1):22-41.

[10] R. Sancibrian, P. Garcia, F. Viadero, A. Fernandez, and A. De-Juan, 2010. "Kinematic design of double-wishbone suspension systems using a multiobjective optimisation approach," *Vehicle System Dynamics*, 48(7):793-813.

[11] H. Habibi, K. H. Shirazi,and M. Shishesaz, 2008. "Roll steer minimization of McPherson-strut suspension system using genetic algorithm method," *Mechanism and Machine Theory*, 43(1):57-67.

[12] P. A. Simionescu and D. Beale, 2002. "Synthesis and analysis of the five-link rear suspension system used in automobiles," *Mechanism and Machine Theory*, 37(9):815-832.

[13] J. K. Eberharter, 2007. "Synthesis of spatial parallel mechanisms with initial conditions using line geometry," *Mechanism and Machine Theory*, 42(10):1289-1297.

[14] H. V. Deo and N. P. Suh, 2004. "Axiomatic design of automobile suspension and steering systems: Proposal for a novel six-bar suspension," *SAE Transactions*, Paper No. 2004-01-0811.

[15] A. P. Morgan and A. J. Sommese, 1987. "A homotopy for solving general polynomial systems that respects m-homogeneous structures," *Applied Mathematics and Computation*, 24(2):101-113.